Sustainable Energy & Fuels

ROYAL SOCIETY OF CHEMISTRY

PAPER

View Article Online
View Journal | View Issue

Cite this: *Sustainable Energy Fuels*, 2022, **6**, 1959

Blend for all or pure for few? Well-to-wheel life cycle assessment of blending electricity-based OME_{3-5} with fossil diesel†

Simon Voelker, [a] Sarah Deutz, [a] Jannik Burre, [b] Dominik Bongartz, [b] Ahmad Omari, [c] Bastian Lehrheuer, [c] Alexander Mitsos, [dbf] Stefan Pischinger, [c] André Bardow [adef] and Niklas von der Assen *[a]

The well-to-wheel environmental impacts of blending electricity-based polyoxymethylene ethers of chain length three to five (OME_{3-5}) with fossil diesel are evaluated, depending on the availability and the environmental impacts of electricity for fuel production. OME_{3-5} is considered a promising substitute and blending component for fossil diesel. We account for the entire life cycle of production, blending, and use of OME_{3-5} with fossil diesel, considering alternative blending ratios and combustion emissions from single-cylinder engine tests. For OME_{3-5} production, our analysis identifies an aqueous route *via* methanol and formaldehyde as the route with the highest exergy efficiency and the lowest environmental impacts among four considered routes. In terms of the carbon footprint of the entire life cycle, diesel-OME_{3-5} blends can only compete with fossil diesel if low-carbon electricity is used for the supply of electricity-based feedstocks and energy. With low-carbon electricity being available, an increased blending ratio of OME_{3-5} with fossil diesel reduces the carbon footprint as well as NO_x and soot emissions. The actual reduction potential additionally depends strongly on the blending ratio. Since low-carbon electricity is limited, it should be used in such a way that environmental impacts are minimal. For the electricity-based fuel OME_{3-5}, this is achieved when distributing OME_{3-5} as a blend component to all fleet vehicles simultaneously instead of switching only a few vehicles to pure OME_{3-5}, *i.e.*, "blend for all" is favorable over "pure for few."

Received 3rd November 2021
Accepted 4th February 2022

DOI: 10.1039/d1se01758f

rsc.li/sustainable-energy

1. Introduction

Today, transportation still depends heavily on the combustion of fossil fuels: By burning fossil fuels, the transport sector of the European Union (EU) accounted for 27% of the EU's total greenhouse gas (GHG) emissions in 2020.[1] Road transportation is responsible for 72% of these transport-related GHG emissions.[1] In cities, road transportation is also one of the main emitters of local air pollutants like nitrogen oxides (NO_x) and soot.[2] Both GHG emissions and local pollutants could be reduced by electrifying road transportation either directly *via* battery electric and fuel-cell vehicles or indirectly *via* electricity-based fuels (e-fuels) for internal combustion engine vehicles. E-Fuels are typically produced from carbon dioxide (CO_2) and hydrogen (H_2) *via* electrolysis thus enabling the indirect integration of renewable electricity into the transport sector.[3]

In current research, CO_2-based polyoxymethylene ethers (OMEs) are considered as promising e-fuels for diesel engines.[4–8] Both as blends with fossil diesel and as full substitutes, OMEs can escape the traditional NO_x-soot trade-off, *i.e.*, both NO_x and soot can be reduced simultaneously.[9] OMEs are commonly distinguished by their chain lengths, of which OME_1 and OME_{3-5} are considered suitable for diesel engines. Although OME_1 shows high potential as a clean e-fuel from a production point of view,[10] it has limitations with regard to the fuel handling and safety classification, *e.g.*, due to its low boiling and flash points.[11] In contrast to OME_1, the production of OME_{3-5} is more energy intensive,[12] but the latter maintains the safety classification of diesel fuel.[9] Substituting fossil diesel with OME_{3-5} is mainly motivated by environmental benefits, which however still need to be proven. To analyze the environmental benefits of OME_{3-5} holistically, a complete life cycle assessment (LCA) of OME_{3-5} as diesel fuel is required. So far, only few studies have been conducted on OME_{3-5}. While all studies confirm that the well-to-wheel GHG emissions largely

[a]*Institute of Technical Thermodynamics, RWTH Aachen University, Aachen 52062, Germany. E-mail: niklas.vonderassen@ltt.rwth-aachen.de*
[b]*Process Systems Engineering, RWTH Aachen University, Aachen 52074, Germany*
[c]*Institute for Combustion Engines, RWTH Aachen University, Aachen 52074, Germany*
[d]*JARA-ENERGY, 52056 Aachen, Germany*
[e]*Energy & Process Systems Engineering, ETH Zurich, Zürich 8092, Switzerland*
[f]*Energy Systems Engineering (IEK-10), Forschungszentrum Jülich, Jülich 52425, Germany*

† Electronic supplementary information (ESI) available. See doi: 10.1039/d1se01758f

depend on the electricity source for e-fuel production, each study focuses on specific phases of the entire OME_{3-5} life cycle or on selected environmental impact categories. Moreover, only one of the studies considers a blend of OME_{3-5} and fossil diesel besides pure OME_{3-5}.

Bokinge *et al.*[13] have conducted a well-to-tank LCA for the carbon footprint of pure OME_{3-5} from biomass gasification as well as of an e-fuel route from CO_2 and H_2. Their study focuses solely on fuel production, while any use-phase emissions from fuel combustion remain uninvestigated.

Hank *et al.*[14] have conducted a well-to-wheel LCA for pure OME_{3-5}. Their study focuses on OME_{3-5} production *via* methanol and formaldehyde (FA) by dehydrogenation of methanol based on the process concept developed by Ouda *et al.*[15–17] Hank *et al.* evaluate the production phase in detail and show that the electricity supply for H_2 production *via* electrolysis has a particularly strong influence on the carbon footprint of fuel production. For fuel combustion, the NO_x emissions of fossil diesel from the LCA database ecoinvent[18] were used for both OME_{3-5} and fossil diesel. Thus, the environmental promises of combustion research are neglected that OMEs enable lower NO_x emissions.[9,11,19] The authors' best-case scenario shows that pure OME_{3-5} can reduce the carbon footprint compared to fossil diesel, while respiratory effects and photochemical ozone formation are the same for both fuels.

Rodríguez-Vallejo *et al.*[20] have compared OME_{3-5} production for multiple energy and raw material sources to fossil diesel in an economic and environmental assessment from well-to-wheel. The production of OME_{3-5} is based on methanol and FA by partial oxidation of methanol. The use phase of OME_{3-5} is based on the study of Hank *et al.*,[14] where only pure OME_{3-5} is analyzed. With these data, Rodríguez-Vallejo *et al.* show that OME_{3-5} can reduce GHG emissions compared to fossil diesel, as expected from previous studies. Contrary to indications from engine measurements,[9] they assume higher NO_x emissions from fuel combustion for OME_{3-5} than for fossil diesel and conclude that OME_{3-5} increases particulate matter and ozone formation compared to fossil diesel. The assumption of higher NO_x emissions from OME_{3-5} combustion may, however, influence their conclusion strongly, since NO_x emissions contribute not only to photochemical ozone formation but also, as a secondary precursor, to particulate matter formation.

Mahbub *et al.*[21] have analyzed the well-to-wheel carbon footprint and soot emissions of OME_{3-5} production from biomass-derived synthesis gas. The study includes the combustion of pure OME_{3-5} and a blend with 10 vol% of OME_{3-5} in fossil diesel on the basis of tests on a chassis dynamometer with a Euro-2 diesel passenger car.[22] Combustion-related NO_x emissions have not been investigated. Mahbub *et al.* state that blending 10 vol% of biomass-derived OME_{3-5} in fossil diesel may reduce GHG and soot emissions by 5% and 30%, respectively, in comparison with fossil diesel.

What is missing entirely so far is a comprehensive well-to-wheel LCA that analyzes (i) actual tailpipe emissions from a driving cycle, in particular the use-phase pollutants NO_x and soot, and (ii) the effect of variable blending ratios of OME_{3-5} in fossil diesel. The blending ratio is defined as the volumetric share of OME_{3-5} within the blended fuel. From a market-perspective, the average blending ratio is limited by the available volume of OME_{3-5}. Still, the blending ratio provides an additional degree of freedom by choosing individual blending ratios, *e.g.*, for individual vehicles within a fleet. One extreme is distributing limited OME_{3-5} as a fixed blend with fossil diesel to the entire fleet ("blend for all"), whereas the opposite extreme is to use OME_{3-5} as a pure fuel in only some vehicles of the fleet ("pure for few"). An environmental assessment of these two extremes is equivalent to the question how limited OME_{3-5} amounts should be allocated within a fleet to minimize environmental impacts. This allocation question is important since electricity-based OME_{3-5} production will be limited by the availability of scarce, clean electricity, which is required to render OME_{3-5} production environmentally favorable according to previous LCA studies.[13,14,20] In fact, the EU's demand for renewable electricity in 2050 due to e-fuel production is estimated to be about eight times bigger than the current annual electricity production in the EU.[23] Using scarce, clean electricity most efficiently in OME_{3-5} production processes is thus crucial. For OME_{3-5} production, several electricity-based routes exist, which should be evaluated to identify those that use limited clean electricity most efficiently and yield minimal environmental impacts.

The goal of this study is to analyze the environmental impacts of OME_{3-5} as full diesel substitute or as diesel blending component in a comprehensive LCA using fossil diesel as benchmark. For this purpose, we integrate NO_x and soot emissions from the combustion of diesel-OME_{3-5} blends for various blending ratios into our analysis: Based on tests from a single-cylinder engine, we simulate a full driving cycle for passenger cars. We further analyze the environmental impacts and exergy efficiency of two anhydrous and two aqueous OME_{3-5} production routes that use CO_2 and H_2 as feedstocks. As anhydrous routes, we consider OME_{3-5} production *via* trioxane and either OME_1 or dimethyl ether (DME). As aqueous routes *via* methanol and FA, we consider FA production by both partial oxidation and dehydrogenation of methanol.

To reflect variabilities and development in the supply chain of feedstocks and energy, we distinguish between a worst-case and a best-case scenario. The worst-case scenario uses the current European power grid mix, today's state-of-the-art technologies for H_2 and heat supply, and CO_2 from direct air capture. In contrast, the best-case scenario uses electricity from wind power, electricity-based technologies for H_2 and heat supply (Power-to-X), and high-purity CO_2 from the chemical industry, *e.g.*, from ethylene oxide or ammonia plants. Finally, we analyze the environmental effect of blending OME_{3-5} gradually into a fleet, depending on the availability of additional electricity and its environmental impacts. We choose the EU fleet of diesel passenger cars as exemplary fleet. Nevertheless, the qualitative results and conclusions of this fleet-wide analysis also apply to other, harder-to-electrify transport subsectors, *e.g.*, long-haul heavy-duty trucks. In particular, we analyze whether limited OME_{3-5} from scarce renewable power should be distributed to the entire fleet as blend, or to selected vehicles as full diesel substitute. In other words, we answer the question

whether we should use identical "blends for all" vehicles or supply "pure OME_{3-5} for few" vehicles in the fleet.

In Section 2, we describe the goal and scope definition of our LCA study and exergy analysis. Section 3 presents the inventory data for the entire life cycle of OME_{3-5} synthesis and combustion, including supply of feedstocks and energy. The resulting environmental impacts of OME_{3-5} as full diesel substitute and as diesel blending component are shown in Section 4. In Section 5, we draw conclusions for policy implications and give recommendations for further research.

2. Life cycle assessment of diesel-OME_{3-5} blends

LCA is a holistic methodology for assessing environmental impacts of product systems along their entire life cycle and is standardized in ISO 14040/14044.[24,25] LCA takes into account and characterizes all environmental impacts of material and energy flows that the product system exchanges with the environment.

2.1. Goal and system boundary

The goal of this LCA is to analyze the environmental impacts of blending the e-fuel OME_{3-5} into a fleet on the example of the EU's fleet of diesel passenger cars. For this goal, we apply a well-to-wheel (cradle-to-grave) system boundary that includes all processes required for OME_{3-5} production, subsequent blending with fossil diesel, and fuel combustion in the engine (Fig. 1, dashed box). Since pure OME_{3-5} and diesel-OME_{3-5} blends are intended to substitute fossil diesel, we benchmark LCA results of the blends to fossil diesel.

For the production phase, we analyze four alternative production routes of OME_{3-5} in more detail, using a well-to-tank (cradle-to-gate) system boundary (Fig. 1, dotted box). All routes for OME_{3-5} production use CO_2-based methanol and FA as intermediates: We consider the two anhydrous routes (1) *via* trioxane and OME_1 (TRI + OME_1) and (2) *via* trioxane and DME (TRI + DME) as well as the two aqueous routes (3) *via* methanol and FA by partial oxidation of methanol (MeOH POX) and (4) *via* methanol and FA by dehydrogenation of methanol (MeOH DEHY). We neglect vehicle construction, road infrastructure emissions, and the fuel distribution because they are likely equal for fossil diesel as well as diesel-OME_{3-5} blends and therefore cancel out in a comparison. The construction of chemical plants for OME_{3-5} production is also neglected due to the lack of data. For the use phase, combustion-related emissions are measured on a single-cylinder engine and subsequently used to simulate the tailpipe emissions for the fuel variants pure fossil diesel, pure OME_{3-5}, and diesel-OME_{3-5}

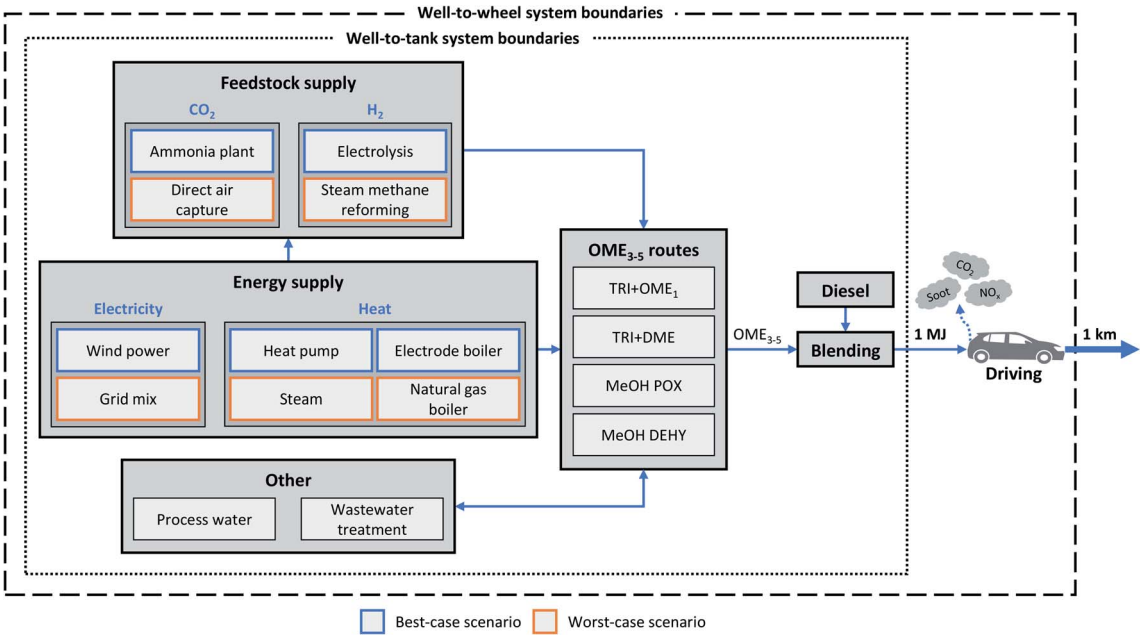

Fig. 1 System boundary of the life cycle of diesel-OME_{3-5} blends. Solid boxes represent production processes, while arrows represent material and energy flows between processes. The dotted arrow indicates use-phase emissions from fuel combustion in the passenger car. The dotted box represents the well-to-tank (cradle-to-gate) system boundary of the OME_{3-5} production and subsequent blending with fossil diesel: The functional unit is "the provision of 1 MJ of enthalpy of combustion" and the reference flow is "1 MJ of enthalpy of combustion." For the well-to-tank system boundary, the use phase of OME_{3-5} is neglected since a constant energy consumption is assumed for the passenger car, making the use phase equal for all routes. The dashed box represents the well-to-wheel (cradle-to-grave) system boundary of the entire life cycle of diesel-OME_{3-5} blends, including fuel combustion with the release of CO_2, soot, and NO_x emissions: The functional unit is "the provision of 1 km of transportation in a medium-size passenger car" and the reference flow is "1 km". Four OME_{3-5} production routes are investigated: OME_{3-5} (1) *via* trioxane and OME_1 (TRI + OME_1), (2) *via* trioxane and DME (TRI + DME), (3) *via* methanol and FA by partial oxidation of methanol (MeOH POX), and (4) *via* methanol and FA by dehydrogenation of methanol (MeOH DEHY). Alternative technologies for the supply of feedstocks and energy are either pre-defined in best- and worst-case scenarios or treated as free optimization variable.

Table 1 Best-case and worst-case scenario in terms of the carbon footprint for the considered technologies. For more details on the underlying LCA datasets see Table S17 in the ESI. DAC: direct air capture, SMR: steam methane reforming

	Best-case	Worst-case
CO_2	Ammonia plant	DAC system
H_2	Electrolysis	SMR
Electricity	Wind power	Grid mix
Heat		
<90 °C	Heat pump	Steam
90–250 °C	Electrode boiler	Steam
>250 °C	Electrode boiler	Natural gas boiler

blends in a driving cycle for passenger cars including an exhaust gas after-treatment system.

We define a best-case and a worst-case scenario in terms of the carbon footprint of diesel-OME_{3-5} blends (Table 1). As previously shown by Hank *et al.*,[14] a best-case scenario with the lowest carbon footprint is achieved with Power-to-X technologies for H_2 and heat supply, combined with renewable electricity and CO_2 from high-purity industrial point sources, *e.g.*, ammonia plants (Fig. 1, blue boxes). We contrast this best-case scenario with a worst-case scenario that considers today's conventional H_2 and heat supply, the average EU grid mix, and CO_2 from direct air capture (Fig. 1, orange boxes). In Section 4.3, the supply chain of diesel-OME_{3-5} blends is optimized for a minimum carbon footprint as function of the carbon footprint of electricity, with the choice among all considered technologies in Table 1 as free optimization variable.

Eventually, we bring the EU fleet of diesel passenger cars into focus by comparing whether "blend for all" or "pure for few" is more favorable from an environmental perspective. For this fleet-wide analysis, introducing OME_{3-5} as "blend for all" can have two effects regarding environmental impact reductions. The first effect is the difference in environmental impacts between pure fossil diesel and diesel-OME_{3-5} blends. The second effect refers to additional, nonlinear synergies from blending OME_{3-5} with fossil diesel, *e.g.*, small blending ratios of OME_{3-5} lead to disproportionately high reductions in combustion emissions (*cf.* Section 3.2). Both effects can be evaluated simultaneously in the relative metric "blending effectiveness factor" (BEF).[10] However, we report results in absolute environmental impacts (*e.g.* g CO_2 eq.) per functional unit (*e.g.* km) to be able to evaluate both effects separately and compare results to common fuel standards. For the "pure for few" case, we use a linear combination of pure OME_{3-5} and pure fossil diesel in analogy to Mancini *et al.*[26]

2.2. Functional unit

Consistent comparisons between production systems require a common basis. In LCA, this common basis for comparing environmental impacts of production systems is the so-called functional unit. The functional unit is a quantitative measure for all functions of a production system. For the detailed analysis of four OME_{3-5} production routes from well-to-tank, we choose "the provision of 1 MJ of enthalpy of combustion" as the functional unit. In the well-to-tank analysis, we neglect the use phase of OME_{3-5} since a constant energy consumption is assumed for the passenger car, making the use phase equal for all four routes. In our well-to-wheel analysis, we choose "the provision of 1 km of transportation in a medium-size passenger car" as the functional unit for comparing different diesel-OME_{3-5} blends to fossil diesel.

2.3. Environmental impact categories

Using diesel-OME_{3-5} blends is mainly motivated by reducing both the impact on climate change of driving a diesel passenger car and the impacts on human health by the local pollutants soot and NO_x from fuel combustion. Therefore, we focus on three environmental impact categories in the life cycle impact assessment (LCIA): climate change in g CO_2 eq., respiratory effects in disease incidence, and photochemical ozone formation in kg NMVOC‡ eq. In the following, we use the term carbon footprint for the impact on climate change. We assess these environmental impact categories according to the LCIA method Environmental Footprint 2.0 (EF 2.0)[27] at midpoint level, as recommended by the Joint Research Centre of the European Commission. Although the use of endpoint indicators is not uncommon in the LCA community, we prefer to present our results at midpoint level for this study. We would like to ensure the comprehensibility of our study for a multi-disciplinary readership that might not be as familiar with the interpretation of endpoint indicators as LCA experts are. Furthermore, methodological uncertainty increases when endpoint instead of midpoint indicators are used.[28] In the EF 2.0 method, the carbon footprint is evaluated following the baseline model of 100 years by the Intergovernmental Panel on Climate Change,[29] respiratory effects are modelled with the particulate matter model recommended by the United Nations Environment Programme,[30] and photochemical ozone formation is assessed with the LOTOS-EUROS model[31] as applied in the LCIA method ReCiPe 2008. Other impact categories are also relevant but beyond the scope of this study.

2.4. Exergy analysis

We conduct an exergy analysis for the OME_{3-5} production to gain a deeper knowledge of the exergy losses and the differences between the four considered OME_{3-5} routes (Fig. 1, well-to-tank). Details regarding the calculation of the exergy efficiency as well as the specific exergies of the considered mass and heat flows are presented in Section S7 in the ESI.†

3. Life cycle inventory for diesel-OME_{3-5} blends

In this section, we describe the inventory data used in our LCA in more detail. First, we describe the anhydrous and aqueous production routes for OME_{3-5} as well as the supply of feedstocks

‡ Non-methane volatile organic compounds.

and energy. Second, we analyze the combustion of diesel-OME_{3-5} blends.

3.1. OME_{3-5} production

All considered routes for OME_{3-5} have two common intermediates: methanol and FA. Following the Power-to-X concept, methanol can be produced by direct CO_2 hydrogenation[32] and is partly used to produce FA in all considered OME_{3-5} routes. Dependent on whether water coexists in the final process step of OME_{3-5} formation, OME_{3-5} routes can be divided into two types: anhydrous and aqueous routes (Fig. 2). In the following, we consider both anhydrous and aqueous routes in our investigation to understand their advantages and drawbacks. All processes are based on similar assumptions and detailed process models created by the respective authors in the simulation software Aspen Plus or CHEMASIM from BASF. For more details on the considered OME_{3-5} production routes and the underlying modelling assumptions see Section S6 in the ESI.† Pinch-based heat integration has been applied for all routes, using the target values for the heating and cooling demand.

Anhydrous routes (TRI + OME_1 and TRI + DME). Anhydrous OME_{3-5} production can either use OME_1 or DME as intermediate (Fig. 2). The concept of OME_{3-5} production *via* trioxane and OME_1 (TRI + OME_1)[33] is based on the work of Burger *et al.*[34] For our study, we use the process models of Bongartz *et al.*[35] and Burre *et al.*[12] that analyzed this process concept in detail. Their process chain considers OME_1 production from H_2 and CO_2 *via* methanol and aqueous FA solution.

For the concept of producing OME_{3-5} from trioxane and DME (TRI + DME), a process similar to OME_{3-5} production *via* the TRI + OME_1 route has been developed and evaluated by Breitkreuz *et al.*,[36] using chemical equilibrium calculations for the reaction and detailed distillation models for the separation part. For the DME production step, we use a model for direct DME production from H_2 and CO_2, using equilibrium-based models for both the reaction and the separation *via* rectification.[37] Methanol, FA, and trioxane production is taken from the TRI + OME_1 route.

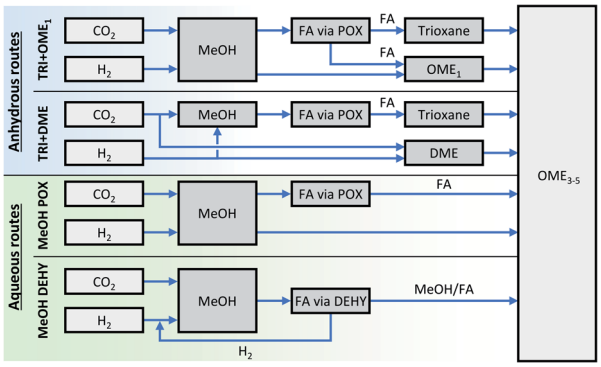

Fig. 2 Flowchart of both anhydrous and both aqueous routes to OME_{3-5}. Boxes represent production processes, while arrows represent material flows between processes. Both anhydrous routes use trioxane (TRI) as an intermediate with either OME_1 (TRI + OME_1) or DME (TRI + DME) as the capping source. Both aqueous routes use methanol (MeOH) and formaldehyde (FA) as intermediates: FA is either produced *via* partial oxidation of methanol (MeOH POX) or *via* dehydrogenation of methanol (MeOH DEHY). In case of the MeOH DEHY route, significant amounts of H_2 are co-produced and thus recycled to the preceding methanol production, reducing the overall H_2 consumption.

Aqueous routes (MeOH POX and MeOH DEHY). In contrast to the anhydrous routes, aqueous routes directly utilize methanol and typically aqueous FA for OME_{3-5} formation (Fig. 2). For the OME_{3-5} route *via* methanol and FA by partial oxidation of methanol (MeOH POX), the process concept is adopted from Held *et al.*[38] with methanol production from H_2 and CO_2.

For the OME_{3-5} route *via* methanol and FA by dehydrogenation of methanol (MeOH DEHY), we combine methanol dehydrogenation with FA absorption in water to selectively separate FA from the gaseous reactor effluent. Thereby, we accept the disadvantage of introducing unfavorable amounts of water into the process: This way, we can use the catalysts and process concept for OME_{3-5} synthesis from methanol and aqueous FA considered by Held *et al.*[38] In principle, it might be possible to synthesize OME_{3-5} from methanol and gaseous FA, which would eliminate the need for FA removal from the gas stream altogether, but this synthesis pathway has only recently been proposed.[39] Ouda *et al.* proposed a similar process concept to the one considered herein, but without introducing water for separating FA from the gaseous reactor effluent, thus potentially benefiting from smaller amounts of water in the process.[17] However, the downstream distillation models used in their work do not account for oligomerisation reactions whose effects on distillation boundaries need to be considered.[40] Therefore, we do not use their results for our analysis but rather those of Held *et al.*,[38] who do use detailed distillation models including these reactions.

In the MeOH DEHY route, we assume a selective separation of H_2 from CO and CH_4 by a membrane for H_2 recycling. For such membranes, high selectivities of up to 1000 and 27 000 have been reported.[41,42] Part of the H_2 is recycled and accumulated in the dehydrogenation reactor to dilute the gaseous methanol feed to the desired 1 : 1 ratio of H_2 to methanol. The rest is recycled to the methanol plant. As the final product, the same ratio of FA to water as in the partial oxidation of methanol is realized such that both can be used for the same proceeding OME_{3-5} process of Held *et al.*[38] See Fig. S7 in the ESI† for a flowsheet of the MeOH DEHY route.

Background data for feedstocks, energy, and others. We also take into account the environmental impacts from technologies providing the feedstocks CO_2 and H_2, electricity, heat, process water and wastewater treatment. For aggregated process datasets, we consider LCA inventories from the GaBi LCA database if datasets are available. Thus, we rely on the ecoinvent LCA database only if LCA inventories are unavailable in GaBi. We do so to ensure that the data basis of our study is as consistent as possible. Furthermore, ecoinvent does not provide a suitable dataset for H_2 from SMR, which we consider in our worst-case scenario (Table 1). The considered technologies are described in the following.

For the CO_2 supply, we consider a direct air capture (DAC) system as well as high-purity sources from the chemical

industry, *e.g.*, ethylene oxide or ammonia plants. In case of the DAC system, CO_2 is captured from the atmosphere. In the atmosphere, CO_2 is much more diluted (410 ppm [43]) than in industrial exhaust streams. Therefore, the energy consumption for capturing CO_2 from the atmosphere is higher, making the DAC system the least efficient technology for CO_2 supply.[44] For the energy requirements of the DAC system, we use the predicted energy targets for industrial DAC plants based on temperature swing adsorption (TSA), according to Deutz *et al.*[45] Note that Madhu *et al.* compared a high-temperature aqueous solution (HT-Aq) DAC to a TSA DAC, and conclude that the TSA DAC outperforms the HT-Aq DAC in all considered impact categories.[46] In current ammonia plants, CO_2 is co-produced during steam reforming of methane and the water–gas shift reaction. In subsequent gas scrubbing, nearly pure CO_2 is separated.[47] Note that the ammonia plant with CO_2 separation is thus a multifunctional product system since it co-produces CO_2 besides ammonia. We therefore apply the avoided burden approach and credit for CO_2 utilization in accordance to Müller *et al.*[48] Since CO_2 is separated in conventional ammonia plants anyway, we attribute the environmental impact of CO_2 capture to the ammonia plant. We model the CO_2 supply from the ammonia plant according to von der Assen *et al.*[44]

H_2 is either supplied by conventional steam reforming from natural gas[49] or a polymer electrolyte membrane (PEM) electrolysis. We model the PEM electrolysis with an overall electricity consumption of 47.6 kW h per kg H_2, representing an overall efficiency of 70%, a water demand of 0.01 m^3 per kg H_2, and an outlet pressure of 30 bar according to Reuβ *et al.*[50] Co-produced oxygen is assumed to be vented to the atmosphere. The construction of the PEM electrolysis is neglected: it accounts for maximum 4% of the total carbon footprint of the PEM electrolysis when renewable electricity is used.[51] Respiratory effects and photochemical ozone formation depend almost exclusively on the electricity supply and are thus not affected by the electrolyser construction. In contrast, the electrolyser construction affects the environmental impact categories ozone depletion and metal depletion that are however beyond the scope of this study.[51]

For electricity supply, we consider the average EU grid mix as well as the average wind electricity of the EU.[49] We also include the country-specific grid mixes of Italy, Denmark, Austria, Finland, Belgium, Switzerland, France, and Norway as well as the average electricity production from photovoltaics and solar-thermal energy in the EU for our analysis of the environmental impacts due to electricity supply.[49] For heat supply, we differentiate between three temperature levels: below 90 °C, between 90 °C and 250 °C, and above 250 °C. Depending on the temperature level, we consider steam production in the chemical industry,[18] natural gas boilers,[49] heat pumps, and electrode boilers. For the heat pump, we assume a coefficient of performance (COP) of 3.28: the COP is averaged from heat pumps built since 2006, with evaporator temperatures between 9–15 °C and condenser temperatures of about 90 °C according to David *et al.*[52] For the electrode boiler, we assume a Power-to-Heat efficiency of 95% according to Müller *et al.*[53]

Additional process data for other processes, *i.e.*, diesel supply, process water supply, and wastewater treatment are taken from the GaBi and ecoinvent LCA databases.[18,49] For the diesel supply, we consider the EU market mix that is provided at a filling station, using the corresponding dataset from the GaBi database.[49] This diesel supply process includes the entire supply chain from drilling through crude oil production and oil refining to transportation to the filling station. The diesel fuel of this dataset contains about 6 wt% of bio-components. The dataset is mainly based on industry data and considers contributions of all delivering countries to the EU fuel mix based on national statistics. More details on the underlying LCA datasets of all processes are listed in Table S17 in the ESI.†

3.2. Diesel-OME_{3-5} blend combustion

The combustion-related raw emissions of diesel-OME_{3-5} blends are characterized by engine tests with a single-cylinder engine (SCE). These SCE tests comprise variations of the exhaust gas recirculation (EGR) rate at different load points with blending ratios of 0 vol%, 20 vol%, 35 vol%, 50 vol%, and 100 vol% OME in fossil diesel as described in previous studies[9,11,54] and additionally new analyses in form of a global design of experiments (DOE) approach. Subsequently, the DOE models are implemented in a mean-value engine model[55,56] (including vehicle, engine, driver, transmission, and after-treatment system) to determine the corresponding vehicular tailpipe emissions in a given driving cycle. Specifications of the SCE, the emission measurement equipment, and the main parameters from the vehicle model are given in Tables S35–S37 in the ESI.†

Within the global DOE test campaign on the SCE, the Worldwide Harmonized Light Vehicles Test Procedures (WLTP) cycle is covered by varying the speed and load range. To include the fuel's effect on the emissions, the DOE is conducted three times namely with pure fossil diesel, with 35 vol% OME_{3-5} in fossil diesel, and with pure OME_{3-5}. A blend with 35 vol% OME_{3-5} generates a sufficient amount of soot that can be measured with high accuracy as required for the DOE. If instead a blend with 50 vol% OME_{3-5} would be used, the soot emissions would be too low to be measured with sufficiently high accuracy. For the subsequent creation of DOE models, 600 points are available in total: The DOE domain covers 40 load points for each considered fuel and 5 variations of calibration parameters per load point on average. The parameters varied in the DOE input domain are given in Table S38 in the ESI.† Subsequently, global DOE models are created from the measured data from the SCE with the ETAS ASCMO software.[57] The measured data is fitted to the DOE input domain by a multiple Gaussian regression analysis procedure within the software.

After evaluating the generated DOE models, we find the trends to be within expectations; in particular, considering that only three fuels have been investigated in the DOE (0 vol%, 35 vol%, and 100 vol% OME_{3-5} in fossil diesel). The observed trends of soot and NO_x emissions are in good agreement with the observations in previous work,[9,11,54] where multiple blending ratios were investigated at different load points. With the generated DOE models, an optimal set of engine calibration

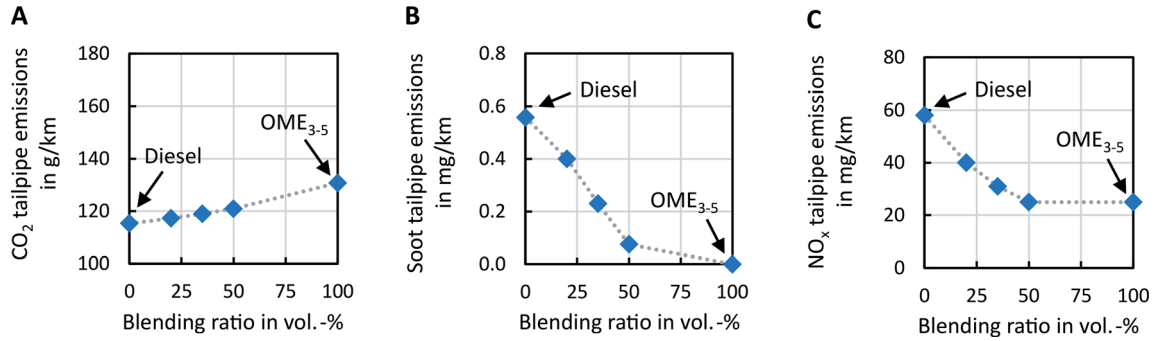

Fig. 3 (A) CO_2, (B) soot, and (C) NO_x tailpipe emissions of diesel-OME_{3-5} blend combustion for various volumetric blending ratios. CO_2 emissions are calculated by the carbon balance for each blending ratio. Soot and NO_x emissions are obtained by single-cylinder engine tests for each blending ratio, using a global design of experiments approach and subsequently simulating a complete driving cycle for a mid-size passenger car.

maps is obtained with the ETAS ASCMO optimizer tool, targeting the best compromise between NO_x, soot, and CO_2 emissions for each fuel. After obtaining the optimized engine calibration maps and the emission models, an in-house transient-capable mean-value engine model is used to simulate the cumulative tailpipe emissions during a WLTP cycle. This WLTP cycle simulation assumes a D-segment passenger car (mid-size vehicle) with a representative rolling resistance curve, a 1.6 liter four-cylinder engine, and an after-treatment system consisting of a diesel oxidation catalyst, a selective NO_x reduction catalyst, and a diesel particulate filter. The resulting tailpipe emissions of CO_2, soot, and NO_x are shown in Fig. 3 and summarized in Table S39 in the ESI.† Note that we expect the qualitative trends of the obtained results to be also valid for other vehicles, *e.g.*, long-haul heavy-duty trucks.

The tailpipe CO_2 emissions increase almost linearly with the OME_{3-5} content (Fig. 3A). This increase in CO_2 emissions is not caused by efficiency losses but is attributed to the fact that OME_{3-5} has a higher specific carbon content per heat of combustion compared to fossil diesel (22 g MJ^{-1} and 20 g MJ^{-1}, respectively).[54] In contrast to CO_2 emissions, soot and NO_x tailpipe emissions reduce nonlinearly with increasing blending ratios of OME_{3-5} in fossil diesel (Fig. 3B and C). Both pollutants are mostly convex functions of the blending ratio except for soot emissions at low blending ratios. Thus, even small blending ratios of OME_{3-5} in fossil diesel drastically reduce both local pollutants soot and NO_x. In contrast to soot, NO_x shows a saturation behavior after about 50 vol% OME_{3-5} content, where an additional increase of OME_{3-5} does not reduce NO_x further. This saturation is attributed to the maximum attainable EGR rate to maintain the relative air–fuel ratio above 1.15 such that efficiency does not deteriorate. An alternative solution to limiting the EGR rate would be the increase of boost pressure, *e.g.*, by means of sophisticated two-stage boosting systems. This system is however beyond the scope of the current work.

For the LCIA in Section 4, we model the emissions from fuel combustion as emitted in the environmental sub-compartment "urban air close to ground". Thereby, we assume driving in an urban environment for which NO_x and soot emissions are characterized with higher, *i.e.*, stricter, characterization factors: For the environmental impact category respiratory effects of the LCIA method EF 2.0, the characterization factors of NO_x and soot emissions in "urban air close to ground" are 6.6 and 78 times higher than in "non-urban air or from high stacks", respectively.

4. Environmental impacts of diesel-OME_{3-5} blends

In this section, we analyze the environmental impacts of diesel-OME_{3-5} blends. First, we identify the most promising route of four OME_{3-5} production routes in a well-to-tank analysis: For this purpose, we conduct exergy analyses and an LCA for the environmental impacts of all routes. Second, we analyze the entire life cycle of diesel-OME_{3-5} blends for various blending ratios from well-to-wheel for the most promising OME_{3-5} route. Third, we analyze the well-to-wheel carbon footprint of the diesel-OME_{3-5} blends depending on the carbon footprint of electricity supply. Finally, we conclude with an analysis of blending OME_{3-5} gradually into a fleet on the example of the EU's fleet of diesel passenger cars, depending on the availability of additional electricity and its environmental impacts.

4.1. Well-to-tank: OME_{3-5} production

Exergy analysis. The exergy flows for producing 1 kg OME_{3-5} of all four OME_{3-5} production routes are visualized in Sankey diagrams in Fig. 4. See Section S8 in the ESI† for numerical results of the exergy analysis.

The largest exergy losses occur in both anhydrous routes (Fig. 4A and B). The overall exergy efficiency is 57% for the TRI + OME_1 route and 55% for the TRI + DME route, with the highest exergy losses occurring due to the high heat demand during trioxane production. Second highest exergy losses occur in the FA production step: These losses are mainly due to the combustion of side products in the off-gas and the conversion of chemical energy to heat in the partial oxidation of methanol. Although the TRI + OME_1 route requires 28 wt% less trioxane than the TRI + DME route, its overall exergy efficiency is only slightly higher: energy losses are higher during OME_1

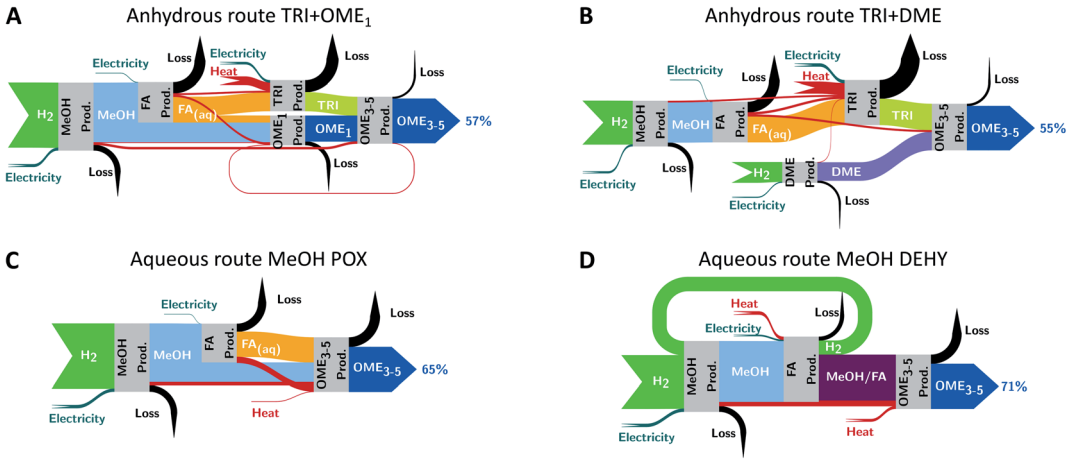

Fig. 4 Sankey diagrams of the exergy analysis for producing 1 kg OME_{3-5}. Boxes represent process steps, whereas arrows denote exergy flows. The presented OME_{3-5} routes are the anhydrous routes *via* (A) trioxane and OME_1 (TRI + OME_1) and *via* (B) trioxane and DME (TRI + DME), as well as the aqueous routes *via* (C) methanol and formaldehyde (FA) by partial oxidation of methanol (MeOH POX) and *via* (D) methanol and FA by dehydrogenation of methanol (MeOH DEHY). The amount of exergy of each mass and energy flow is represented by the width of the arrow.

production than during DME production, reducing the advantage of a lower trioxane demand for the TRI + OME_1 route.

The aqueous routes MeOH POX and MeOH DEHY yield overall exergy efficiencies of 65% and 71%, respectively (Fig. 4C and D). For the MeOH POX route, the largest exergy losses occur during FA and OME_{3-5} production. In contrast, the MeOH DEHY route benefits twofold from the significant co-production of H_2. First, less side products are produced and thus burned during FA production, reducing its exergy losses. Second, the H_2 recycle to the preceding methanol production reduces the overall H_2 demand and thereby increases the overall exergy efficiency.

The exergy analysis of both anhydrous routes and aqueous routes shows that the MeOH DEHY route results in the highest overall exergy efficiency and uses H_2 most efficiently.

LCA. The well-to-tank environmental impacts of the four OME_{3-5} production routes are shown in Fig. 5 for the best-case scenario. See Fig. S1 in the ESI† for the worst-case scenario.

From a well-to-tank perspective, all routes have negative carbon footprints in the best-case scenario since CO_2 emitted otherwise from the CO_2 source ammonia plant is avoided. However, for the carbon footprint, we additionally indicate the end-of-life of OME_{3-5} as hatched area to emphasize that the full life cycle of OME_{3-5} is no carbon sink: All carbon is eventually released again as CO_2 during fuel combustion, making CO_2-based OME_{3-5} carbon-neutral at best, but only if carbon-neutral electricity is used for fuel production and all other supply chains are also carbon-neutral.

In the best-case scenario, already very low-carbon electricity from wind power is used, leading to almost carbon-neutral OME_{3-5} production. All routes have nearly identical life-cycle carbon footprints of about 7 g CO_2 eq. per MJ (Fig. 5A). Although both aqueous routes MeOH POX and MeOH DEHY require more CO_2 and thereby benefit from higher credits for CO_2 utilization, they also have higher CO_2 purge streams compared to both anhydrous routes. Additionally, the H_2 recycle of the MeOH DEHY route results in the lowest H_2 demand and thus in the lowest overall electricity consumption because H_2 is supplied *via* PEM electrolysis in this scenario. However, the benefit of the more efficient H_2 usage is rather low in terms of the carbon footprint in the best-case scenario: Electricity is supplied by wind power with an already low carbon footprint, making the efficient usage of electricity less important for the overall carbon footprint. Nevertheless, a high efficiency in H_2 and electricity usage is beneficial in order to keep the demand for low carbon electricity as low as possible.

In terms of respiratory effects and photochemical ozone formation (Fig. 5B and C), the aqueous routes MeOH POX and MeOH DEHY have the lowest environmental impacts. Both impact categories are almost exclusively dominated by the upstream impacts of electricity supply: electricity is mostly used for the Power-to-X technologies PEM electrolysis, heat pumps, and electrode boilers, followed by OME_{3-5} production and CO_2 supply. The MeOH DEHY route shows the lowest H_2 consumption due to the H_2 recycle from the FA production to the preceding methanol production. This benefit is, however, partly offset by a higher heat consumption during FA and OME_{3-5} production compared to the MeOH POX route.

Consequently in the best-case scenario, respiratory effects and photochemical ozone formation are more decisive for the choice of the route than the carbon footprint since the carbon footprints are almost equal.

In the worst-case scenario (Fig. S1†), the differences between the four routes are greater in all considered impact categories than in the best-case scenario, and both aqueous routes MeOH POX and MeOH DEHY show the lowest environmental impacts. Note that we considered a TSA DAC in the worst-case scenario, which performs better than a HT-Aq DAC, according to Madhu *et al.*[46] We thus expect our results to worsen slightly if we would instead assume a HT-Aq DAC. In this scenario, H_2 is supplied by conventional steam methane reforming, resulting in high contributions to the overall carbon footprint (Fig. S1A†). In

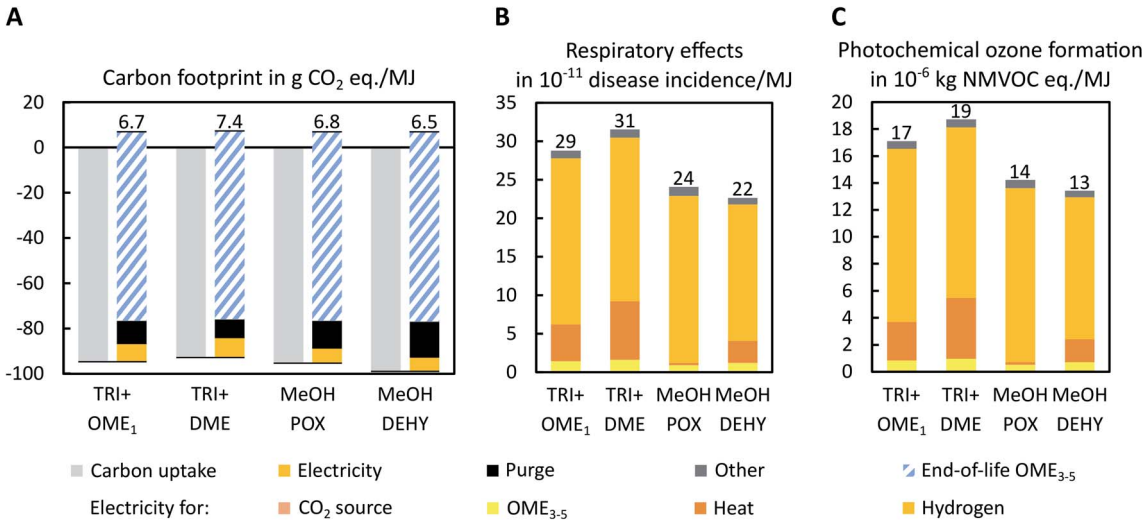

Fig. 5 Well-to-tank (A) carbon footprint in g CO_2 eq. per MJ, (B) respiratory effects in 10^{-11} disease incidence per MJ, and (C) photochemical ozone formation in 10^{-6} kg NMVOC eq. per MJ of the four OME_{3-5} production routes for the best-case scenario. The carbon footprint of the carbon uptake due to CO_2 utilization is negative (light grey). Positive environmental impacts result from direct CO_2 emissions in purge gases from OME_{3-5} production (black), minor emissions due to process water supply and wastewater treatment (dark grey), and electricity supply (yellow). The electricity supply is further subdivided in electricity for hydrogen, heat, OME_{3-5}, and CO_2 supply in (B) and (C). Note however that environmental impacts due to electricity for CO_2 supply are very small and thus barely visible. Although not inside the system boundary of a well-to-tank analysis, we additionally indicate the end-of-life emissions from OME_{3-5} combustion for the carbon footprint (A, hatched blue): the entire life cycle of CO_2-based fuels cannot be carbon-negative and is thus carbon-neutral at best. The same figure is shown with CO_2 from DAC in the best-case scenario in Section S2 in the ESI.†

terms of the carbon footprint, the aqueous routes MeOH POX and MeOH DEHY benefit from a lower heat consumption compared to both anhydrous routes. Respiratory effects and photochemical ozone formation are both dominated by the fossil-based supply of heat in the worst-case scenario (Fig. S1B and C†). Although the MeOH DEHY route still profits from a lower H_2 consumption due to its H_2 recycle, its higher heat consumption affects the environmental impacts more strongly in the worst-case scenario. Consequently, in contrast to the best-case scenario, the MeOH DEHY route has higher environmental impacts than the MeOH POX route in the worst-case scenario.

All in all, the aqueous routes MeOH POX and MeOH DEHY yield the lowest environmental impacts in both the worst-case (Fig. S1†) and the best-case scenario (Fig. 5). In the proceeding well-to-wheel analysis of diesel-OME_{3-5} blends, we focus on the aqueous MeOH DEHY route as it has the highest overall exergy efficiency of all four routes in addition to its environmental advantages (Fig. 4D). Note though that considering exergy efficiency alone is not sufficient to rank the OME_{3-5} routes in terms of environmental impacts: While the MeOH DEHY route has the highest exergy efficiency, it shows lower environmental impacts in the best-case scenario and higher ones in the worst-case scenario compared to the MeOH POX route.

4.2. Well-to-wheel: the entire life cycle of diesel-OME_{3-5} blends

Fig. 6 shows the well-to-wheel analysis of diesel-OME_{3-5} blends for the best-case scenario: Investigated fuel blends are pure diesel, 20, 35 and 50 vol% OME_{3-5} in fossil diesel as well as pure OME_{3-5} (*cf.* Section 3.2). Over the entire life cycle, diesel-OME_{3-5} blends can reduce not only the carbon footprint but also respiratory effects and photochemical ozone formation compared to fossil diesel (Fig. 6). These results partly contradict earlier findings that OME_{3-5} performs worse than fossil diesel in terms of particulate matter and photochemical ozone formation.[20] However, in this previous study,[20] NO_x emissions of OME_{3-5} combustion[14] are assumed to be one order of magnitude higher than those of fossil diesel combustion.[58] In contrast to the previous study, OME_{3-5} combustion has actually shown to enable large reductions of NO_x emissions compared to fossil diesel in current literature.[9,19] This discrepancy may influence the authors' findings strongly since NO_x emissions contribute not only to photochemical ozone formation but also, as a precursor, to respiratory effects. Our findings are in line with recent literature from OME combustion showing the combustion benefits of OME_{3-5}. In any case, this highlights the necessity to use measured combustion emissions as reliable data basis for LCA studies.

In terms of the carbon footprint, the combustion, *i.e.*, use phase, of the fuels contributes most to the overall impact in the best-case scenario (Fig. 6A). Note that the combustion of OME_{3-5} slightly increases CO_2 emissions compared to fossil diesel due to the lower heating value (*cf.* Section 3.2). However, the production of OME_{3-5} overcompensates increased CO_2 emissions from fuel combustion, reducing the overall carbon footprint of the entire life cycle: Blending ratios of 20, 35 and 50 vol% OME_{3-5} in fossil diesel reduce the carbon footprint by

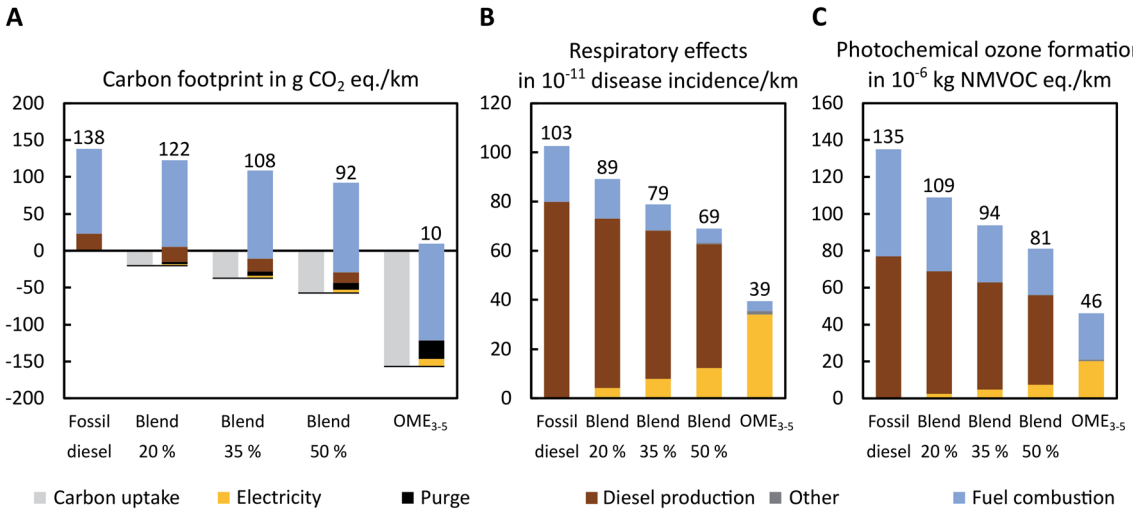

Fig. 6 Well-to-wheel (A) carbon footprint in g CO_2 eq. per km, (B) respiratory effects in 10^{-11} disease incidence per km, and (C) photochemical ozone formation in 10^{-6} kg NMVOC eq. per km of pure fossil diesel, blends of OME_{3-5} in fossil diesel, and pure OME_{3-5} for the best-case scenario. OME_{3-5} is produced *via* the MeOH DEHY route. The carbon footprint of the carbon uptake due to CO_2 utilization is negative (light grey). Positive environmental impacts result from electricity supply (yellow), direct CO_2 emissions in purge gases from OME_{3-5} production (black), diesel production (brown), fuel combustion (light blue), and minor emissions due to process water supply and wastewater treatment (dark grey). The same figure is shown with CO_2 from DAC in the best-case scenario in Section S4 in the ESI.†

12%, 22% and 33%, respectively. Pure OME_{3-5} reduces the carbon footprint by 93%. Respiratory effects are dominated by the production of fossil diesel and, for increasing blending ratios, also by the electricity supply (Fig. 6B). Blending 20, 35 and 50 vol% OME_{3-5} with fossil diesel reduces respiratory effects by 14%, 23% and 33%, respectively, while pure OME_{3-5} reduces respiratory effects by 62%. In terms of photochemical ozone formation, fuel combustion and diesel production are the most important contributors (Fig. 6C). Photochemical ozone formation reduces by 19%, 30% and 40%, due to the blending of 20, 35 and 50 vol% OME_{3-5} in fossil diesel, respectively. Pure OME_{3-5} reduces photochemical ozone formation by 66%.

In the worst-case scenario (Fig. S3†), all environmental impact categories increase strongly with increasing blending ratios because fossil-based technologies are considered instead of wind power and the Power-to-X technologies of the best-case scenario (*cf.* Section 2.1). The largest increase is thus found for pure OME_{3-5} for which the carbon footprint increases by 161%, respiratory effects by 409%, and photochemical ozone formation by 199%. Note though that diesel-OME_{3-5} blends would still reduce the local tailpipe emissions of NO_x and soot (*cf.* Section 3.2). Technological choices for electricity, H_2, and heat supply are therefore crucial and further investigated in the proceeding analysis.

4.3. Blending OME_{3-5} gradually into a fleet

The preceding well-to-wheel analysis for the best-case and worst-case scenario highlights that Power-to-X technologies and low-carbon electricity are decisive to realize environmental benefits of diesel-OME_{3-5} blends. In Fig. 7, we therefore minimize the carbon footprint of the supply chain of diesel-OME_{3-5} blends for the MeOH DEHY route as function of the carbon footprint of electricity supply. In this optimization, technological choices in the supply chain depend solely on the carbon footprint of electricity supply since we do not predefine any scenario-specific technology sets (*cf.* Section 2.1).

Below a carbon footprint of electricity supply of 360 g CO_2 eq. per kW h, heat supply between 90 and 250 °C changes from steam production in the chemical industry to electrode boilers, while heat supply above 250 °C changes from natural gas to electrode boilers below 235 g CO_2 eq. per kW h. H_2 supply changes from fossil-based steam methane reforming to PEM electrolysis below 227 g CO_2 eq. per kW h. As a result, the production system is solely based on Power-to-X technologies below 227 g CO_2 eq. per kW h. Consequently, further reducing the carbon footprint of electricity supply strongly reduces the well-to-wheel carbon footprint of pure OME_{3-5} (Fig. 7, strongly negative slope). The well-to-wheel carbon footprints of diesel-OME_{3-5} blends and pure OME_{3-5} are lower than that of pure fossil diesel, once the carbon footprint of electricity supply is below 140 g CO_2 eq. per kW h.

An even more ambitious electricity carbon footprint of 45 g CO_2 eq. per kW h or lower is required if OME_{3-5} is to comply with the European Commission's renewable energy directive II (RED II).[59] In the RED II, fuels from non-biological origin, *e.g.*, e-fuels, shall reduce GHG emissions by at least 70% compared to a fossil fuel comparator (Fig. 7, dotted horizontal line). See Section S5 in the ESI† for the same analysis recalculated for CO_2 from DAC instead of an ammonia plant. Our recalculations show that the cleaner the electricity supply the less sensitive are the environmental impacts towards the considered CO_2 supply, *e.g.*, different DAC systems such as TSA or HT-Aq DAC.

Reducing the well-to-wheel carbon footprint with diesel-OME_{3-5} blends is thus only possible if Power-to-X technologies

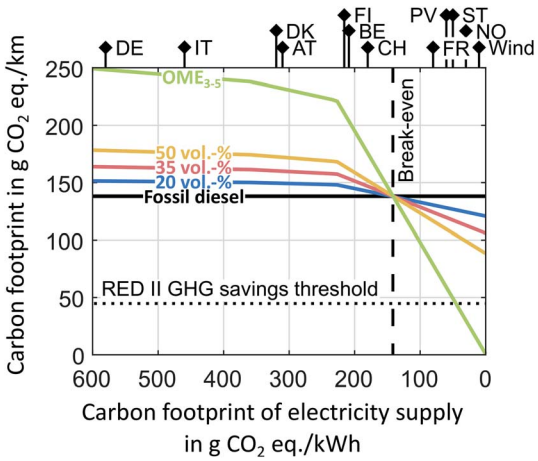

Fig. 7 The well-to-wheel carbon footprint as function of the carbon footprint of electricity supply for pure OME_{3-5}, blends of 20, 35, and 50 vol% OME_{3-5} in diesel as well as pure fossil diesel. The well-to-wheel impacts include emissions along the entire life cycle of diesel-OME_{3-5} blends. Note that pure fossil diesel is a horizontal line since aggregated process data from the GaBi LCA database is used. Thereby, changes due to the decarbonization of electricity and electrification of the refinery cannot be reflected. In reality, the line of pure fossil diesel would thus slightly decrease if electricity is decarbonized and heat supply is electrified. The theoretical lower bound of fossil diesel would be 115 g CO_2 eq. per km, with diesel combustion being the only contributor, if fossil diesel production would be carbon-neutral (*cf.* Fig. 6A). Note though that the curves of diesel-OME_{3-5} blends would then also decrease slightly. Various country- and technology-specific carbon footprints of electricity supply are shown at the top as solid verticals. The dashed vertical line represents the break-even carbon footprint of electricity supply below which diesel-OME_{3-5} blends reduce the well-to-wheel carbon footprint compared to fossil diesel. The dotted horizontal line represents the GHG savings threshold from the renewable energy directive II (RED II) of the European Commission. The RED II states that GHG emissions savings from fuels of non-biological origin shall be at least 70% compared to a fossil fuel comparator with 94 g CO_2 eq. per MJ [59] corresponding to 148 g CO_2 eq. per km with an energy consumption of 1.57 MJ per km. CO_2 is supplied by an ammonia plant. See Section S5 in the ESI† for the same figure with CO_2 from DAC. Abbreviations are as follows: DE for Germany, IT for Italy, DK for Denmark, AT for Austria, FI for Finland, BE for Belgium, CH for Switzerland, FR for France, PV for photovoltaic, ST for solar-thermal, NO for Norway, and wind for wind power.

for heat and H_2 supply are combined with low-carbon electricity. For example, today's country-specific grid mixes of France and Norway as well as wind and photovoltaic power would already enable reducing the well-to-wheel carbon footprint with diesel-OME_{3-5} blends. However in the future, such low-carbon electricity will also be demanded by competing Power-to-X applications and will remain scarce. Environmental impact reductions of diesel-OME_{3-5} blends will therefore depend on both the availability of additional electricity for OME_{3-5} production and the environmental impacts of that electricity supply.

In the following, we further analyze this dependence in more detail on the example of the EU's current fleet of diesel passenger cars. In this analysis, we focus on those electricity supply grid mixes and technologies that showed the potential to reduce the carbon footprint compared to fossil diesel in the preceding supply chain optimization. We determine the current annual mileage of the EU fleet of diesel passenger cars as 1.34 trillion km: today, the EU fleet of diesel passenger cars amounts to about 95.7 million cars,[60] while the average annual mileage by EU passenger cars is estimated as 14 000 km.[23] We assume this mobility demand with diesel-like passenger cars to be constant. For this estimated mobility demand, we then calculate the blending ratio of OME_{3-5} in fossil diesel, depending on additionally available electricity for OME_{3-5} production. This blending ratio corresponds to distributing diesel-OME_{3-5} blends for the entire EU fleet of diesel passenger cars ("blend for all"). For more details on the calculations see Section S11 in the ESI.†

Fig. 8 shows the volumetric blending ratio, the carbon footprint, respiratory effects, and photochemical ozone formation as function of additionally available electricity for OME_{3-5} production. The aforementioned impact categories are evaluated for different technology- and country-specific grid mixes for electricity supply as well as for the theoretical limit of a burden-free electricity supply. The solid curves show the environmental impacts of diesel-OME_{3-5} blends for the entire fleet ("blend for all"), while the dashed lines represent the linear combination of using pure fossil diesel and pure OME_{3-5} in the fleet ("pure for few"). We show "pure for few" only for one electricity supply for the sake of better readability.

The blending ratio of OME_{3-5} in diesel is a concave nonlinear function of the additional electricity supply (Fig. 8A). This concave function results from OME_{3-5} being no direct substitute for fossil diesel since OME_{3-5} has a lower specific heating value than fossil diesel: Substituting 1.0 L of fossil diesel requires 1.8 L of OME_{3-5} to provide the same amount of enthalpy of combustion. Therefore, more OME_{3-5} is required than fossil diesel is replaced, resulting in an increase of the total fuel mass for increasing blending ratios. Using pure OME_{3-5} for the entire fleet, *i.e.*, a blending ratio of 100 vol%, would require 1.3 PW h of additional electricity to substitute the entire EU diesel demand for passenger cars. This additional demand corresponds to almost half of the 2.8 PW h of electricity currently produced in the EU states.[61]

The well-to-wheel carbon footprint of diesel-OME_{3-5} blends depends linearly on the amount of additional electricity (Fig. 8B). Thus, each additional unit of electricity for OME_{3-5} production has the same marginal impact on the overall carbon footprint irrespective of the blending ratio. Consequently for the carbon footprint, there would be no difference between blending the produced OME_{3-5} with fossil diesel for the entire fleet ("blend for all") and switching only some vehicles to pure OME_{3-5} usage instead ("pure for few").

In contrast to the carbon footprint, the well-to-wheel respiratory effects and photochemical ozone formation of diesel-OME_{3-5} blends depend nonlinearly on the amount of additional electricity (Fig. 8C and D): In the use phase of diesel-OME_{3-5} blends, NO_x and soot emissions reduce nonlinearly with increasing blending ratios (*cf.* Section 3.2). For respiratory effects and photochemical ozone formation, the curves of "blend for all" are always below the lines of "pure for few," *i.e.*, "blend for all" has always less environmental impacts than

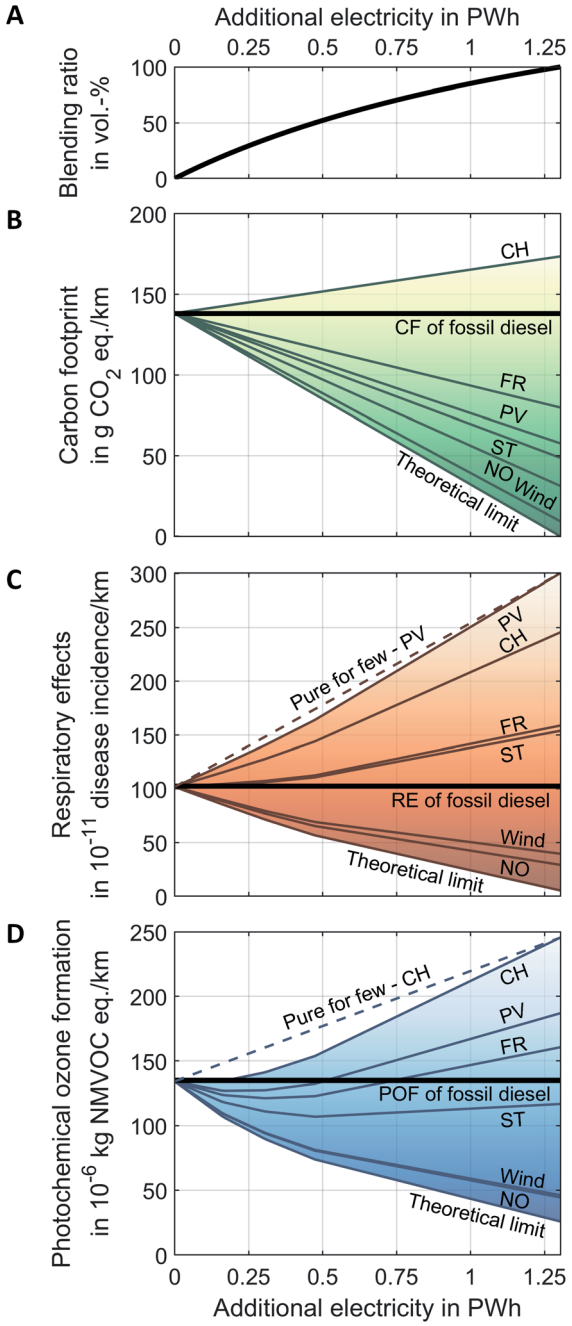

Fig. 8 (A) The volumetric blending ratio, the well-to-wheel (B) carbon footprint (CF), (C) respiratory effects (RE), and (D) photochemical ozone formation (POF) as function of additionally available electricity for OME_{3-5} production. Results are presented for country- and technology-specific environmental impacts of electricity. Solid curves indicate the environmental impacts of blending OME_{3-5} with fossil diesel for the entire fleet ("blend for all"), while dashed lines show the results for switching only some diesel passenger cars to pure OME_{3-5} usage ("pure for few"). "Pure for few" is the linear combination of pure diesel and pure OME_{3-5} and is, for the sake of better readability, shown for only two examples. The black bold lines indicate the environmental impacts of pure fossil diesel for reference. CO_2 is supplied by an ammonia plant. See Section S5 in the ESI† for the same figure with CO_2 from DAC. CH: Switzerland, FR: France, NO: Norway, PV: photovoltaic, and ST: solar-thermal. The theoretical limit of a burden-free electricity supply is also included as lower bound.

"pure for few." Consequently, blending OME_{3-5} gradually with fossil diesel for the entire fleet ("blend for all") is always better than switching only some vehicles to pure OME_{3-5} usage ("pure for few"). We discuss the significantly higher environmental impacts for electricity from photovoltaic compared to electricity from wind power in Section S12 in the ESI.†

The benefit of "blend for all" over "pure for few" is maximal at a blending ratio of 50 vol% for both respiratory effects and photochemical ozone formation with higher benefits for photochemical ozone formation. This blending ratio of 50 vol% requires 0.47 PW h of electricity for OME_{3-5} production. Moreover, we find that the cleaner the electricity supply (*cf.* Fig. 7, top axis for exemplary values), the greater the benefit of "blend for all" over "pure for few." When applying "blend for all" instead of "pure for few," photochemical ozone formation reduces by 12% with Swiss (CH) electricity and by 21% with Norwegian (NO) electricity at a blending ratio of 50%. Similarly, respiratory effects reduce by 7% with Swiss (CH) electricity and by 13% with Norwegian (NO) electricity.

Consequently, blending OME_{3-5} with fossil diesel for the entire fleet can contribute to reducing the carbon footprint, photochemical ozone formation, and respiratory effects compared to pure fossil diesel. However, fuel suppliers should always distribute OME_{3-5} as a blend with fossil diesel to the filling stations to maximize the environmental benefits for the entire fleet. The blending ratio should then be gradually increased, when more additional electricity is available for OME_{3-5} production. Besides the availability of electricity, the reductions in each environmental impact category depend also on the environmental impacts of electricity supply. Today, electricity from wind power and the Norwegian electricity grid mix are already sufficiently clean to reduce all three environmental impact categories with diesel-OME_{3-5} blends simultaneously (Fig. 8).

For contribution analyses of "blend for all" in Fig. 8 for various country- and technology-specific electricity supplies, see Fig. S12–S18 in the ESI.†

5. Conclusion

Based on life cycle assessment (LCA), we analyze the well-to-wheel environmental impacts of blending electricity-based OME_{3-5} with fossil diesel for various blending ratios. For this purpose, we investigate four alternative production routes and integrate measured NO_x and soot emissions from diesel-OME_{3-5} blend combustion for various blending ratios. For OME_{3-5} production, our exergy analysis and well-to-tank LCA indicate that both aqueous routes are preferable: The exergy efficiency of the aqueous route *via* methanol and formaldehyde by dehydrogenation of methanol is the highest with 71%, while both aqueous routes also have the lowest environmental impacts in both scenarios. Future studies should thus aim at improving and establishing routes *via* the dehydrogenation of methanol, such as that proposed by Ouda *et al.*[17] and the variant considered herein.

Our well-to-wheel LCA for the entire life cycle shows that blending OME_{3-5} with fossil diesel can reduce environmental

impacts for all considered impact categories in the best-case scenario. Therefore, our results contradict earlier findings for respiratory effects and photochemical ozone formation.[20] We thus emphasize to use measured combustion emissions as reliable data basis for future LCA studies of any e-fuel to derive reliable conclusions. In our best-case scenario, most emissions arise during fuel combustion in terms of the carbon footprint. The major cause for respiratory effects is diesel production. Photochemical ozone formation is mostly caused by diesel production and fuel combustion. Note though that burden-shifting to other impact categories may occur that have not been considered in our study: Hank *et al.* point out that "freshwater eutrophication" and "resources use, minerals and metals" are exceeded strongly for electricity-based OME_{3-5}, *e.g.*, due to the construction of wind turbines and photovoltaic panels that demand large amounts of minerals and metals.[14] In the worst-case scenario with fossil-based technologies for H_2 and heat supply, all considered environmental impacts increase, rendering e-fuels worse than fossil diesel. We systematically show that the well-to-wheel carbon footprint of e-fuels like diesel-OME_{3-5} blends is strongly dependent on the carbon footprint of electricity supply, which is in line with the findings of previous studies.[10,13,14,20]

In the coming decades, low-carbon electricity will probably remain scarce since it is likely also demanded by competing Power-to-X technologies. For this reason, we compare the environmental effect of gradually blending OME_{3-5} into an entire fleet ("blend for all") to switching only some vehicles to pure OME_{3-5} usage ("pure for few"). We demonstrate this fleet-wide analysis exemplary for the EU fleet of diesel passenger cars, emphasizing that we expect the qualitative results and conclusions to be also valid for other transport subsectors, *e.g.*, long-haul heavy-duty trucks, which are more difficult to electrify and thus require synthetic fuels to maintain long driving ranges. Our results show that increasing blending ratios of OME_{3-5} in the EU fleet of diesel passenger cars can contribute to reducing the carbon footprint, photochemical ozone formation, and respiratory effects compared to fossil diesel. Reduction potentials depend however strongly on the environmental impacts of electricity supply, the desired blending ratio, and the availability of additional electricity for OME_{3-5} production.

We further show that it is always environmentally favorable to blend OME_{3-5} with fossil diesel for the entire fleet ("blend for all") rather than using pure OME_{3-5} only in few vehicles ("pure for few"). For minimal environmental impacts, fuel suppliers should thus distribute OME_{3-5} as a blend component to the filling stations and gradually increase the blending ratio as soon as more electricity is available for OME_{3-5} production. However, for a blending ratio of 100 vol% OME_{3-5} to be used in all diesel passenger cars, we estimate that almost half of the EU's current electricity generation would be required in addition to the current generation. Yet, the blending ratio would likely increase over time for a constant amount of electricity for OME_{3-5} production: With battery electric vehicles on the rise, the demand for fossil diesel fuel by the remaining diesel vehicles is likely to decrease in the future. Our analysis can assist in designing environmentally efficient strategies to gradually increase the market share of e-fuel blends, *e.g.*, diesel-OME_{3-5} blends, for a decreasing amount of vehicles with internal combustion engines. However, the resulting environmental impacts of such e-fuel blends should also be benchmarked to battery electric vehicles in future studies. In such studies, integrated assessment models could be used to forecast the decreasing demand for fossil diesel.

Apart from electricity-based OME_{3-5}, we further recommend to extend the scope to blends of bio-fuels and other e-fuel candidates in future studies. In case of bio-fuels, the limited availability of biomass needs to be additionally analyzed in detail. The study of Rodríguez-Vallejo *et al.* indicates that OME_{3-5} from bio-based methanol might perform slightly better than electricity-based OME_{3-5} in terms of the carbon footprint and worse in terms of other impact categories that are particularly relevant for bio-based products, *e.g.*, land use and terrestrial eutrophication.[20] Consequently, bio-based OME_{3-5} does not perform better or worse than electricity-based OME_{3-5} *per se*. A sound comparison of bio- and CO_2-based OME_{3-5} requires therefore a comprehensive LCA of both, including reliable use-phase emissions and also exergy efficiency as additional metric.

Unlike passenger cars, other transport subsectors are more difficult to electrify: Light- and heavy-duty trucks are, besides aviation and shipping, also responsible for large amounts of GHG emissions and are likely to depend on liquid energy carriers for the coming decades. We expect that the qualitative trends and conclusions of our results are also valid for light and heavy-duty trucks. E-Fuels such as OME_{3-5} therefore have the potential to play an important role in both decarbonizing the transport sector and reducing the impacts on human health of NO_x and soot emissions.

Author contributions

S. V., S. D., A. B., and N. V. designed the concept of the study. S. V., S. D. conducted the life cycle assessment under supervision of N. V. and wrote the corresponding sections. J. B. developed the process concept of the OME_{3-5} route *via* methanol and formaldehyde by dehydrogenation of methanol. J. B., D. B. analyzed the production processes in terms of exergy efficiency under supervision of A. M. and wrote the corresponding sections. A. O. carried out the engine tests to obtain the combustion emissions and simulated the driving cycle emissions under supervision of S. P. A. O. and B. L. wrote the corresponding sections. S. V. took the lead in writing the manuscript and wrote all other sections. All authors provided critical feedback and contributed to the discussions as well as revision of the manuscript.

Conflicts of interest

There are no conflicts to declare.

Acknowledgements

S. V.'s, B. L.'s, A. B.'s, and N. A.'s work was performed as part of the Cluster of Excellence EXC2186 "The Fuel Science Center,"

which is funded by the Deutsche Forschungsgemeinschaft (DFG, German Research Foundation) under Germany's Excellence Strategy (ID 390919832). S. D.'s, J. B.'s, D. B.'s, A. O.'s, S. P.'s, A. B.'s, and A. M.'s work was performed as part of the Kopernikus Project P2X: Flexible use of renewable resources – exploration, validation and implementation of "Power-to-X" concepts (FKZ 03SFK2A), which is funded by the German Federal Ministry of Education and Research (BMBF). S. D.'s, J. B.'s, A. B.'s, and A. M.'s work was also performed as part of the project NAMOSYN: Nachhaltige Mobilität durch synthetische Kraftstoffe (FKZ 03SF0566P0), which is funded by the German Federal Ministry of Education and Research (BMBF). We thank the three anonymous reviewers whose valuable feedback helped to improve and clarify our manuscript.

References

1 European Environment Agency, *Annual European Union greenhouse gas inventory 1990–2018 and inventory report 2020: Submission to the UNFCCC Secretariat*, Copenhagen, Denmark, 2020.
2 European Environment Agency, *Air quality in Europe: 2018 report, EEA report No 12/2018*, Publications Office of the European Union, Luxembourg, 2018.
3 S. Schemme, R. C. Samsun, R. Peters and D. Stolten, *Fuel*, 2017, **205**, 198.
4 J. Artz, T. E. Müller, K. Thenert, J. Kleinekorte, R. Meys, A. Sternberg, A. Bardow and W. Leitner, *Chem. Rev.*, 2018, **118**(2), 434.
5 C. J. Baranowski, A. M. Bahmanpour and O. Kröcher, *Appl. Catal., B*, 2017, **217**, 407.
6 K. Hackbarth, P. Haltenort, U. Arnold and J. Sauer, *Chem. Ing. Tech.*, 2018, **90**(10), 1520.
7 R. Sun, I. Delidovich and R. Palkovits, *ACS Catal.*, 2019, **9**(2), 1298.
8 J. Burre, D. Bongartz, S. Deutz, C. Mebrahtu, O. Osterthun, R. Sun, S. Völker, A. Bardow, J. Klankermayer, R. Palkovits and A. Mitsos, *Energy Environ. Sci.*, 2021, **14**(2), 3686.
9 A. Omari, B. Heuser, S. Pischinger and C. Rüdinger, *Appl. Energy*, 2019, **239**, 1242.
10 S. Deutz, D. Bongartz, B. Heuser, A. Kätelhön, L. Schulze Langenhorst, A. Omari, M. Walters, J. Klankermayer, W. Leitner, A. Mitsos, S. Pischinger and A. Bardow, *Energy Environ. Sci.*, 2018, **11**(2), 331.
11 A. Omari, B. Heuser and S. Pischinger, *Fuel*, 2017, **209**, 232.
12 J. Burre, D. Bongartz and A. Mitsos, *Ind. Eng. Chem. Res.*, 2019, **58**(14), 5567.
13 P. Bokinge, S. Heyne and S. Harvey, *Energy Sci. Eng.*, 2020, **8**(7), 2587.
14 C. Hank, L. Lazar, F. K. Mantei, M. Ouda, R. J. White, T. Smolinka, A. Schaadt, C. Hebling and H.-M. Henning, *Sustainable Energy Fuels*, 2019, **3**(11), 3219.
15 M. Ouda, G. Yarce, R. J. White, M. Hadrich, D. Himmel, A. Schaadt, H. Klein, E. Jacob and I. Krossing, *React. Chem. Eng.*, 2017, **2**(1), 50.
16 M. Ouda, F. K. Mantei, M. Elmehlawy, R. J. White, H. Klein and S.-E. K. Fateen, *React. Chem. Eng.*, 2018, **3**(3), 277.
17 M. Ouda, F. Mantei, K. Hesterwerth, E. Bargiacchi, H. Klein and R. J. White, *React. Chem. Eng.*, 2018, **3**(5), 676.
18 G. Wernet, C. Bauer, B. Steubing, J. Reinhard, E. Moreno-Ruiz and B. Weidema, *Int. J. Life Cycle Assess.*, 2016, **21**(9), 1218.
19 G. Richter and H. Zellbeck, *Motortech. Z.*, 2017, **78**(12), 66.
20 D. F. Rodríguez-Vallejo, A. Valente, G. Guillén-Gosálbez and B. Chachuat, *Sustainable Energy Fuels*, 2021, **5**(9), 2504.
21 N. Mahbub, A. O. Oyedun, A. Kumar, D. Oestreich, U. Arnold and J. Sauer, *J. Cleaner Prod.*, 2017, **165**, 1249.
22 L. Pellegrini, M. Marchionna, R. Patrini and S. Florio, in *SAE Technical Paper Series*, SAE International400 Commonwealth Drive, Warrendale, PA, United States, 2013.
23 S. Siegemund, M. Trommler, O. Kolb and V. Zinnecker, *E-fuels study: The potential of electricity-based fuels for low-emission transport in the EU: An expertise by LBST and dena*, Deutsche Energie-Agentur GmbH (dena), Berlin, 2017.
24 International Organization for Standardization, *ISO 14040: Environmental Management: Life Cycle Assessment: Principles and Framework*, 2006.
25 International Organization for Standardization, *ISO 14044: Environmental Management: Life Cycle Assessment: Requirements and Guidelines*, 2006.
26 N. D. Mancini and A. Mitsos, *Phys. Chem. Chem. Phys.*, 2011, **13**(48), 21351.
27 European Commission and PEFCR Guidance document, *Guidance for the development of Product Environmental Footprint Category Rules (PEFCRs)*, version 6.3, May 2018.
28 M. Z. Hauschild and M. A. J. Huijbregts, *Life Cycle Impact Assessment*, Springer, Dordrecht, 2015.
29 T. F. Stocker, D. Qin, G.-K. Plattner, M. M. B. Tignor, S. K. Allen, J. Boschung, A. Nauels, Y. Xia, V. Bex and P. M. Midgley, *Climate Change 2013: The Physical Science Basis. Contribution of Working Group I to the Fifth Assessment Report of the Intergovernmental Panel on Climate Change*, Cambridge University Press, Cambridge, United Kingdom and New York, NY, USA, 2014.
30 P. Fantke, J. Evans, N. Hodas, J. Apte, M. Jantunen, O. Jolliet and T. E. McKone, in *Global Guidance for Life Cycle Impact Assessment Indicators*, ed. R. Frischknecht and O. Jolliet, Paris, 2016, vol. 1.
31 R. van Zelm, M. A. J. Huijbregts, H. A. den Hollander, H. A. van Jaarsveld, F. J. Sauter, J. Struijs, H. J. van Wijnen and D. van de Meent, *Atmos. Environ.*, 2008, **42**(3), 441.
32 É. S. Van-Dal and C. Bouallou, *J. Cleaner Prod.*, 2013, **57**, 38.
33 N. Schmitz, J. Burger, E. Ströfer and H. Hasse, *Fuel*, 2016, **185**, 67.
34 J. Burger, M. Siegert, E. Ströfer and H. Hasse, *Fuel*, 2010, **89**(11), 3315.
35 D. Bongartz, J. Burre and A. Mitsos, *Ind. Eng. Chem. Res.*, 2019, **58**(12), 4881.
36 C. F. Breitkreuz, N. Schmitz, E. Ströfer, J. Burger and H. Hasse, *Chem. Ing. Tech.*, 2018, **90**(10), 1489.
37 D. Bongartz, L. Doré, K. Eichler, T. Grube, B. Heuser, L. E. Hombach, M. Robinius, S. Pischinger, D. Stolten, G. Walther and A. Mitsos, *Appl. Energy*, 2018, **231**, 757.

38 M. Held, Y. Tönges, D. Pélerin, M. Härtl, G. Wachtmeister and J. Burger, *Energy Environ. Sci.*, 2019, **12**(3), 1019.
39 A. Grünert, P. Losch, C. Ochoa-Hernández, W. Schmidt and F. Schüth, *Green Chem.*, 2018, **20**(20), 4719.
40 N. Schmitz, E. Ströfer, J. Burger and H. Hasse, *Ind. Eng. Chem. Res.*, 2017, **56**(40), 11519.
41 N. W. Ockwig and T. M. Nenoff, *Chem. Rev.*, 2007, **107**(10), 4078.
42 A. K. Prabhu and S. T. Oyama, *J. Membr. Sci.*, 2000, **176**(2), 233.
43 R. J. H. Dunn, D. M. Stanitski, N. Gobron and K. M. Willett, *Bull. Am. Meteorol. Soc.*, 2020, **101**(8), S9–S127.
44 N. von der Assen, L. J. Müller, A. Steingrube, P. Voll and A. Bardow, *Environ. Sci. Technol.*, 2016, **50**(3), 1093.
45 S. Deutz and A. Bardow, *Nat. Energy*, 2021, **6**, 203.
46 K. Madhu, S. Pauliuk, S. Dhathri and F. Creutzig, *Nat. Energy*, 2021, **6**(11), 1035.
47 J. C. M. Farla, C. A. Hendriks and K. Blok, *Clim. Change*, 1995, **29**(4), 439.
48 L. J. Müller, A. Kätelhön, S. Bringezu, S. McCoy, S. Suh, R. Edwards, V. Sick, S. Kaiser, R. Cuéllar-Franca, A. El Khamlichi, J. H. Lee, N. von der Assen and A. Bardow, *Energy Environ. Sci.*, 2020, **13**(9), 2979.
49 GaBi, *GaBi 9.2.0.58: Software-System and Database for Life Cycle Engineering, DB 8.7 - SP 39*, thinkstep AG, Leinfelden-Echterdingen, Germany, 2019.
50 M. Reuß, T. Grube, M. Robinius, P. Preuster, P. Wasserscheid and D. Stolten, *Appl. Energy*, 2017, **200**, 290.
51 K. Bareiß, C. de La Rua, M. Möckl and T. Hamacher, *Appl. Energy*, 2019, **237**, 862.
52 A. David, B. V. Mathiesen, H. Averfalk, S. Werner and H. Lund, *Energies*, 2017, **10**(4), 578.
53 L. J. Müller, A. Kätelhön, M. Bachmann, A. Zimmermann, A. Sternberg and A. Bardow, *Front. Energy Res.*, 2020, **8**, 1.
54 A. Omari, *Characterization of Polyoxymethylen Dimethyl Ether for Diesel Engine Applications*, PhD thesis, Aachen, 2021, in press.
55 S.-Y. Lee, J. Andert, D. Neumann, C. Querel, T. Scheel, S. Aktas, M. Miccio, J. Schaub, M. Koetter and M. Ehrly, *SAE Int. J. Engines*, 2018, **11**(6), 1479.
56 S.-Y. Lee, J. Andert, S. Pischinger, M. Ehrly, J. Schaub, M. Koetter and A. S. Ayhan, *SAE Technical Paper Series 2019-01-0195*, 2019.
57 ASCMO, *Data-based Modeling and Model-based Calibration*, ETAS, 2016.
58 A. Simons, *Int. J. Life Cycle Assess.*, 2016, **21**(9), 1299.
59 European Commission, *Directive (EU) 2018/2001 of the European Parliament and of the Council of 11 December 2018 on the promotion of the use of energy from renewable sources*, 2018.
60 Eurostat, *Passenger cars in the EU*, https://ec.europa.eu/eurostat/statistics-explained/index.php/Passenger_cars_in_the_EU, last accessed January 2021.
61 Eurostat, *Electricity production, consumption and market overview*, https://ec.europa.eu/eurostat/statistics-explained/index.php/Electricity_production, consumption_and_market_overview, last accessed January 2021.